

# Dry Lubricated Rolling-Sliding Contact – Operation Behavior and Calculation of Local Frictional Energy

Sebastian Sklenak, Jens Brimmers and Christian Brecher

## Initiation and Motivation

For numerous reasons, the tooth contact in a power-transmitting gearbox, which is subjected to high mechanical loads, is usually designed as an oil-lubricated contact (Fig. 1). In this case, the oil film on the contact surfaces is intended to create a separation between the base and counter body [Ref. 1]. The separation of the contact surfaces results from the elastohydrodynamic lubricating film buildup, which is created by the tangential velocity between the two tooth flanks. The lubricating film reduces the stress in the contact zone and is thus intended to prevent tooth flank damage, such as micropitting, pitting and scuffing [Refs. 2–3]. In addition to reducing friction, one of the lubricant’s main tasks is to dissipate the frictional heat generated in tooth contact. Other advantages of liquid lubricants are the removal of wear particles generated by abrasive wear in the tooth contact and the corrosion protection of the gear surfaces.

However, for certain operating conditions and environments, liquid lubrication of gear drives is not possible or can only be implemented with great restrictions or at high cost (Fig. 1). In the food industry, guidelines specify the handling of hazardous operating materials, such as lubricants, in machines [Ref. 4]. Accordingly, the use of liquid lubricants requires the design of complex sealing systems and continuous checks of the lubricated assemblies, so that fluid-free rolling-sliding contact can be an alternative solution for this application. In the aerospace industry, the use of lubricating oils and greases is limited due to the extreme operating conditions. These include in particular

the large temperature and pressure range to which the lubricant is exposed during its service life. These extreme operating conditions lead to outgassing in many greases and oils, which in turn leads to changes in the operating properties of the lubricant. Due to the high system reliability required in the aerospace industry, the use of lubricating oils and greases is often excluded [Ref. 5]. Furthermore, from an economic point of view, the type of lubrication plays a role in the design of a gearbox. Considerable costs are incurred for the design and maintenance of the lubrication system as well as for the purchase and disposal of the lubricant (Fig. 1).

Due to an interruption in the lubricant supply, the gearing in Figure 1 exhibits severe deformation of the teeth of both gears. The discoloration on the face of the gearing indicates overheating of the material, so that the resulting reduction in strength leads to failure of the gearing. Investigations into the interruption of the lubricant supply show that conventional gears do not achieve running times close to those of conventional applications when subjected to high mechanical loads [Ref. 6]. For applications where lubrication with oil or grease cannot be guaranteed or is not feasible, solid lubricant systems offer an alternative for reducing power loss. However, the structure of the dry tribological system differs from that of conventional lubrication systems, so that, for example, there is no lubricant circuit for dissipating the power loss. This means that precise knowledge of the tribological mechanisms is required, especially for the optimization of dry rolling-sliding contacts with high mechanical

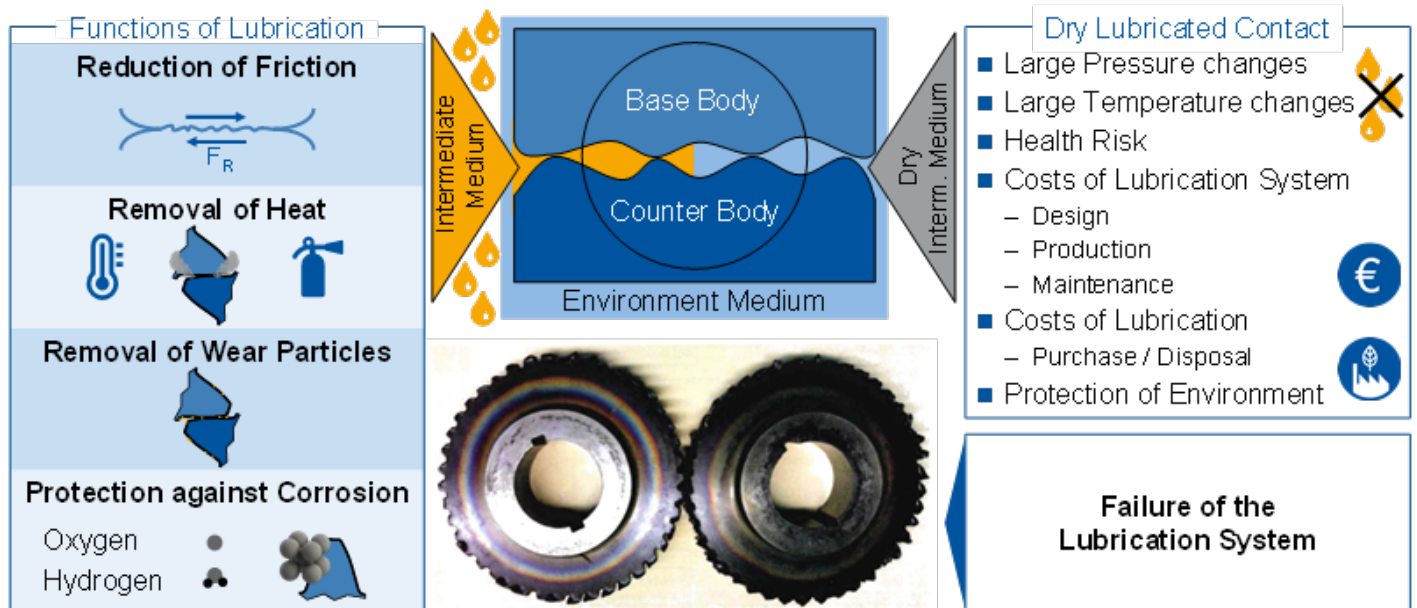


Figure 1 Functions of lubricant in a rolling contact and applications for dry lubrication [Ref 6].

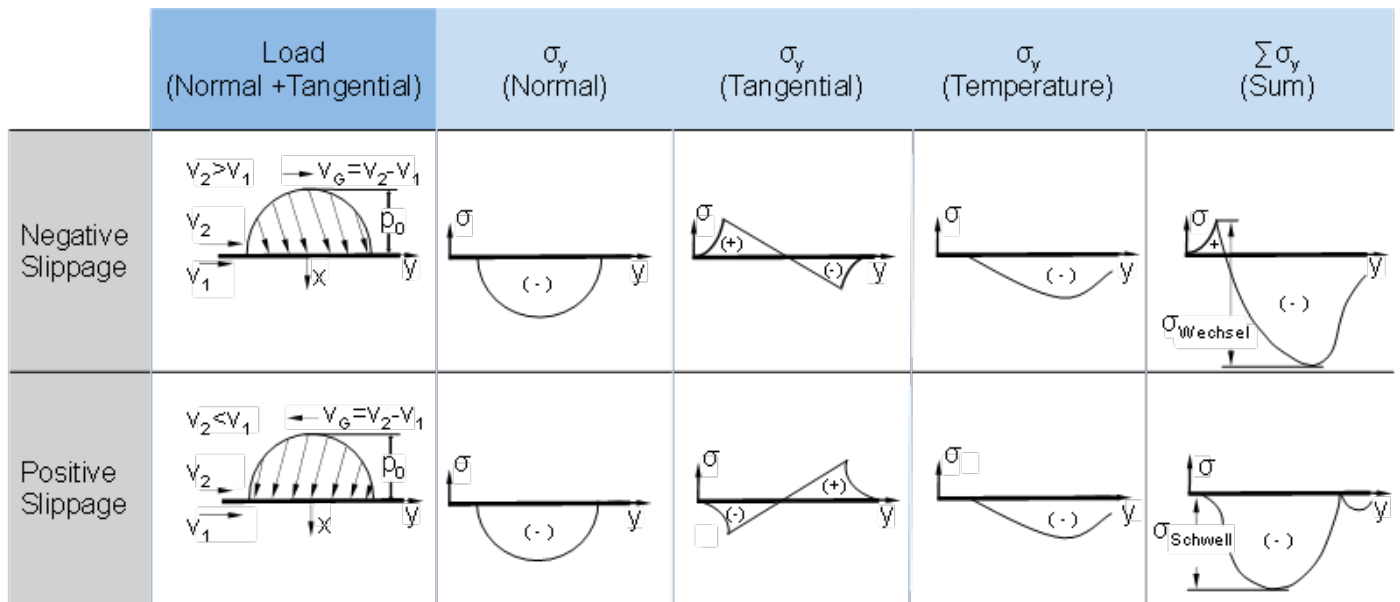


Figure 2 Stresses due to dry lubricated rolling contact [Ref. 1].

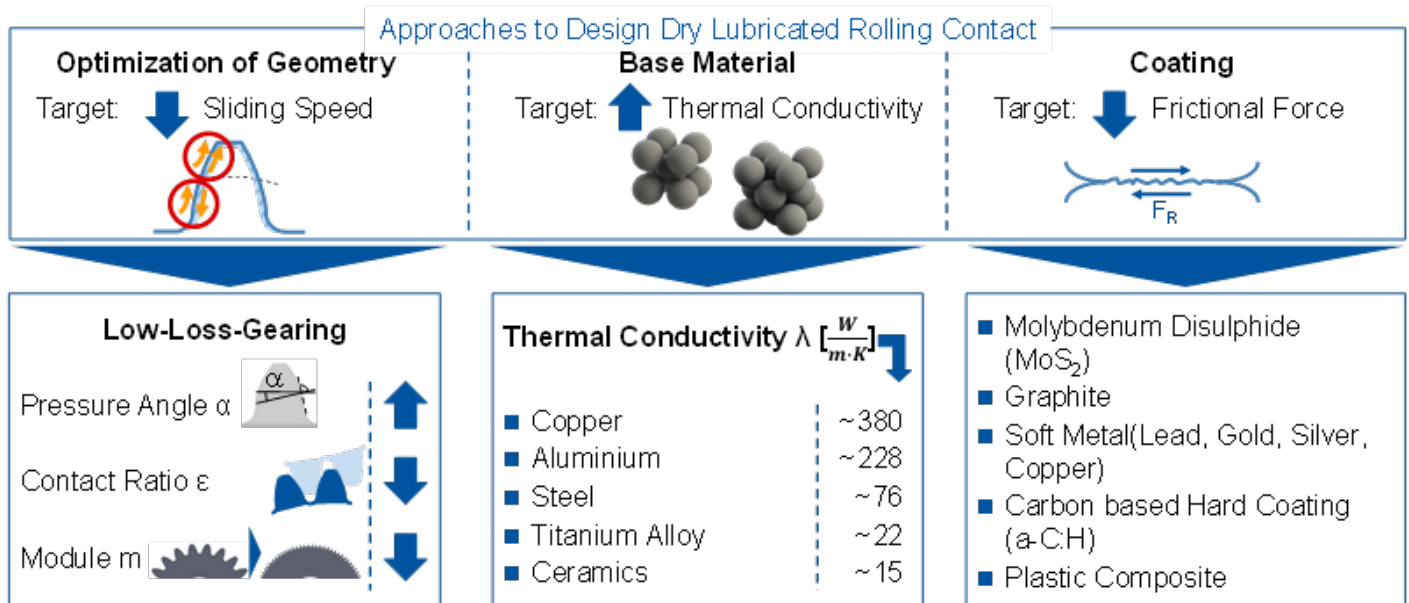


Figure 3 Approaches for dry lubricated rolling-sliding contacts [Refs. 10–11].

loads. The transfer and action mechanisms in dry rolling-sliding contacts are the subject of current research in the priority program DFG SPP 2074 of the German Research Foundation DFG.

### State of the Art

In dry rolling-sliding contact, the stress on the macroscopic contact surface is composed of the three local components of normal force (pressure distribution), tangential force (friction force distribution) and temperature (thermal expansion). In the sum of the three components, the stress component parallel to the direction of sliding accounts for the largest proportion of the total stress state [Ref. 1]. Figure 2 compares the individual distributions of the three components for the equivalent stress  $\sigma_y$  for negative and positive slip, respectively. It is clear that the maximum stress amount of the individual components does not differ between negative and positive slip. However, the sum of stresses for negative slip compared to positive slip shows a larger

and changing stress, so that the contact area has an increased risk of failure due to the more critical stress.

For a design of the gears in dry and mechanically highly loaded rolling-sliding contact with a long service life, three different approaches are pursued separately and in combination with each other (Fig. 3). With the aid of a loss-optimized gear geometry, the sliding velocities of the tooth flanks can be reduced, so that the thermal stress is reduced and the wear behavior is improved [Refs. 7–8]. Loss-optimized gears (so-called low-loss gears) are characterized by a large pressure angle, a small profile overlap and the smallest possible module (low tooth height) [Ref. 8]. Changing the base material for gears influences the dry running properties. In addition to high-alloy steels [Ref. 5] and aluminum and titanium alloys [Ref. 9], plastics [Ref. 3] are also used for dry gear stages. Ceramic materials are already used for dry rolling-sliding bearings in high-temperature applications. However, ceramics are unsuitable as a base

material for gear applications due to the high tensile strength required and especially due to the shock-like stress peaks in tooth meshing [Ref. 3].

As a third starting point for an optimized design of dry rolling-sliding contacts, solid lubricants are used in the form of a coating (Fig. 3). The use of solid lubricants can lead to a reduction in stress due to a reduced frictional force and lower thermal expansion. Among solid lubricants, PTFE has one of the lowest coefficients of friction for both static and sliding friction. However, PTFE has a relatively low thermal operating range compared to other solid lubricants, such as soft metals [Ref. 11]. Soft metals, such as lead, gold, silver, and copper, are used for rolling contacts in rolling bearings due to their low coefficient of friction and good thermal resistance [Ref. 11].

In the field of investigation, the use of single and multi-layer carbon-based coating systems for lubricated tooth contact to reduce stress and wear has already been analyzed in detail [Refs. 12–13]. The work of Brecher shows that PVD coatings have a significant effect on the frictional behavior and load carrying capacity of gears and rolling-sliding contacts [Refs. 12–13]. Investigations on dry ball-on-disk contact with diamond-like carbon coatings show a strong dependence of the displacement and friction coefficients on humidity. In experimental investigations of the mass temperature and coefficient of friction in dry rolling-sliding contact, the influence of slip was considered for a carbon-based hard coating and a molybdenum disulfide coating [Ref. 14]. The slip was increased in stages in analogy to the test procedure for the scuffing load capacity DIN ISO 14635 [Ref. 15]. In deviation from DIN ISO 14635, the load changes for each stage are non-uniform and dependent on the change in mass temperature. Analysis of the tests showed that the frictional properties improve compared with the uncoated and unlubricated rolling-sliding contact, but do not reach the magnitude of an oil-lubricated rolling contact.

Kropp investigates dry tooth contact for various combinations of material and coating [Ref. 16]. The number of load-cycles-per-load level deviates from the standardized test procedure for scuffing. Analysis of the test results shows that the base material of the test specimens has an influence on the service life of the coating [Ref. 16]. However, no clearly better combination of

coating system and base material could be observed here compared to the usual gear steel 16MnCr5. The results show that further investigations of other combinations of coating and substrate material are necessary to achieve a significant improvement compared to the usual gear steel.

Increased coating thickness and reduced roughness can increase the service life of carbon coated tooth flanks [Ref. 7]. Studies on the service life of coated gear flanks show no increased service life for variants that were smoothed with a running-in process before applying the coating [Ref. 3]. In addition to the coatings, the condition after production and the residual cooling lubricant from production can also influence the frictional behavior and load capacity of oil-lubricated gears [Ref. 17]. It is questionable how the influences of manufacturing, such as different surface structures and residual cooling lubricant, affect dry rolling-sliding contact.

In summary, it can be seen for the tooth contact that the stress in the dry rolling-sliding contact differs significantly from the stress in the oil-lubricated rolling-sliding contact. There are approaches to implementing and investigating dry gear applications, but the mechanisms of action have not yet been researched to the same extent as is the case with oil-lubricated gear applications.

### Objective and Approach

The state of the art shows that dry operation with conventional gears is not feasible for many applications. The reduction in service life is related to the increased power loss, so that the question arises as to how the frictional force behaves in dry rolling-sliding contact and how the surface structure affects the distribution of the local frictional energy. The aim of this report is to gain knowledge of the frictional force behavior in dry rolling-sliding contact and to calculate the time-variable pressure distribution and local frictional energy for different orientations of the surface structure (Fig. 4).

Extending the scope of existing standards usually requires extensive experimental investigation of the areas of the standards to be extended (Fig. 4). The experimental investigation requires a uniform test concept and a defined damage criterion. Initial preliminary tests will be used to investigate the influences

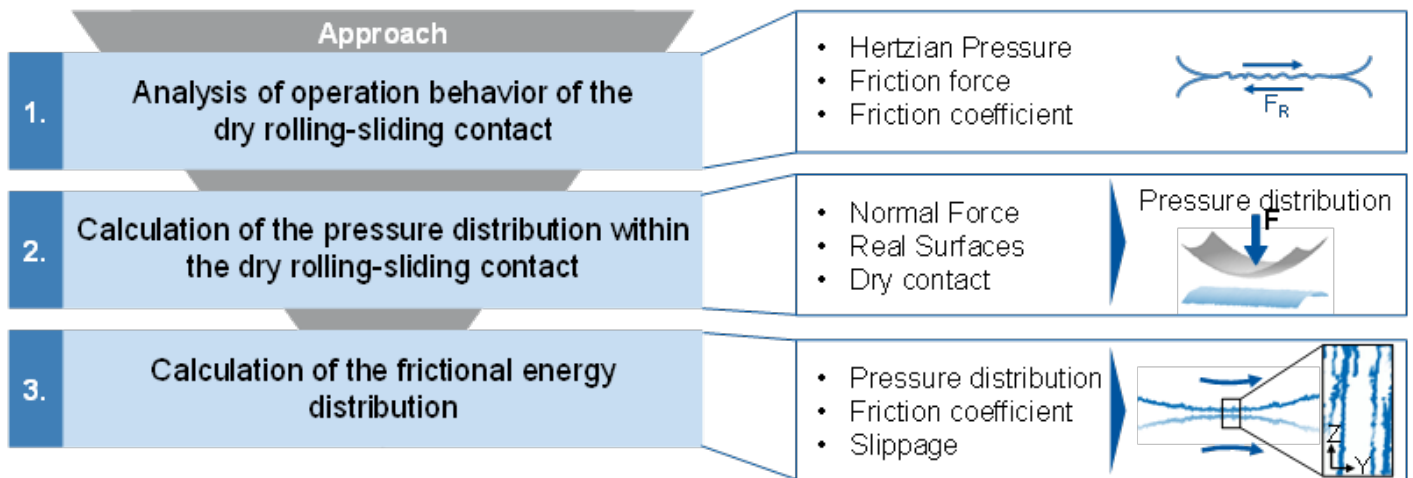


Figure 4 Objective and approach.

### Test Parameter

$t_i$	= 120 s
$\Delta F_{\text{stage}}$	= 463 N
$F_{\text{run in}}$	= 45 N
$s_{\text{test shaft}}$	= -11.2 %
$n_{\text{test}}$	= 339 min <sup>-1</sup>
$n_{\text{counter}}$	= 377 min <sup>-1</sup>
$Ra_{\text{test}}$	= 0.90 μm
$Ra_{\text{counter}}$	= 0.21 μm

### Test Condition

Point contact  
Coating: a-C:H:W  
Dry lubrication

### Friction Coefficient $\mu$

$$\mu = \frac{F_R}{F_N}$$

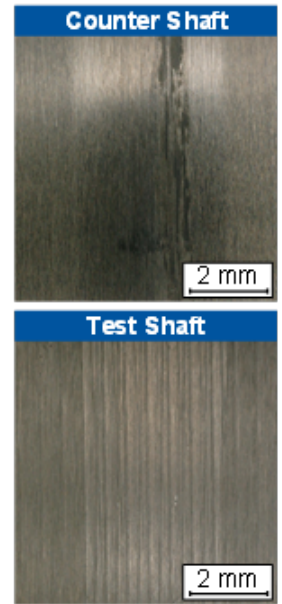
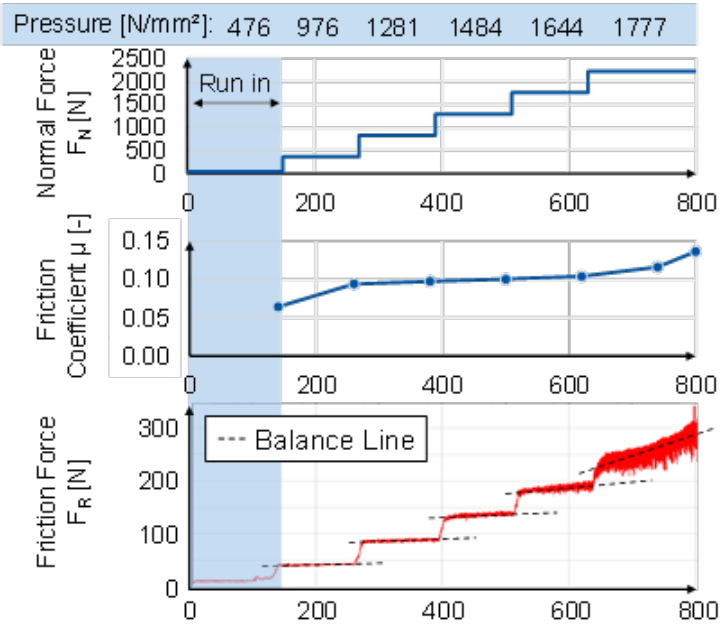


Figure 5 Pre-test pressure ramp-up with dry lubricated rolling-sliding contact.

on the service life and the operational behavior regarding friction force of the dry rolling-sliding contact.

In the dry contact of rough surfaces, a large number of micro-contacts are created, so that the apparent macroscopic contact area is limited to a smaller real area [Refs. 18–19]. Thus, a calculation method for the temporal, high-resolution and large-area pressure distribution within a load cycle is required for the investigation of the effective mechanisms in the dry contact (Fig. 4). For the theoretical investigation of the influence of different orientations of the surface structure on the time-varying pressure distribution, the rolling-sliding contact between rough surfaces with a micro structure either transversely and/or longitudinally to the sliding direction is calculated and analyzed. Based on a variable pressure distribution, the local frictional energy will be calculated and analyzed for 3 different variants.

## Experimental Investigation of Dry Lubricated Rolling-Sliding Contact

The first preliminary tests on dry rolling-sliding contact at the WZL friction force tribometer were used to investigate whether the existing test concepts and test parameters for investigating oil-lubricated contacts can be transferred to dry contact. The test procedure used is a staged pressure run-up analogous to the test procedure for scuffing damage. If the damage criterion is not met, the pressure is increased by one stage for a constant motor speed after an interval  $t_i$ . The damage criterion is defined as a sudden increase in the frictional force or the maximum frictional force or a strong subjective noise increase. Figure 5, for example, shows the friction force curve of a test between two a-C:H:

W-coated surfaces. The test was interrupted after the fifth load level due to a strong increase in the frictional force. The frictional force curve shows a constant average frictional force with little scatter at the first levels. As the load level increases, the balancing grades in the friction force diagram show that the friction force increases despite the constant normal force. The

reason for the increase in the coefficient of friction is assumed to be a relationship between the increasing test specimen temperature and the continuous coating wear during the test run. A subsequent analysis of the running surfaces of the test and counter shafts revealed a coating failure (Fig. 5).

Furthermore, the preliminary tests show that the friction force tribometer is suitable for investigating the dry rolling-sliding contact. This is shown, among other things, by the necessary load range of the normal force, which is smaller for dry tests than for oil-lubricated tests, but is covered by the load range that can be mapped in the test rig. In the macroscopic form of the pressure distribution, a distinction can be made between a point contact and a line contact. For the dry contact, the preliminary tests indicate better repeatability for the line contact. When varying the interval duration, it can be seen that tests with a short interval duration of  $t_i = 120$  s tend to achieve a higher pressing level compared to those with a long interval duration of  $t_i = 1200$  s. For the influence of the interval duration, it is suspected that the lower number of load cycles lead to less wear in the contact area and that a short interval duration results in a lower mass temperature compared to a long interval duration. When using the test procedure for the oil-lubricated rolling-sliding contact, it is particularly important to maintain a constant interval duration because of the influence on the pressure level that can be achieved. In addition, the scatter of test results is higher than for oil-lubricated rolling-sliding contact. Repeat tests are therefore necessary for a systematic investigation of the dry rolling-sliding contact.

In summary, it can be stated that a maximum temperature, or a temperature change, or a maximum frictional force can be defined as a damage criterion and thus as an abortion criterion for the experimental test on dry rolling contact. Due to the influence of temperature, comparability between tests with different speeds of the test shaft is not possible. The analogous test procedure for the frictional load capacity is a suitable test concept for the experimental investigation of the dry rolling-sliding

contact.

### Contact Calculation within the Disk-on-Disk-Contact

Depending on the manufacturing process used, different surface structures arise on the contact surface which deviate from an ideally smooth surface, so that the real microscopic contact surface is composed of the contact of many individual roughness peaks [Refs.18–19]. The combination of individual micro-contact points and a relative speed of the two contacting surfaces results in a varying local pressure within a load change [Ref.20]. Due to the influence of thermal effects on the wear behavior in the dry rollingsliding contact, the local pressing process is crucial for a wear or service life prediction. For a better understanding of the tribological mechanisms in dry rollingsliding contact, the influence of different orientation of the surface structure on the temporal change of the pressure distribution is investigated with the aid of a calculation model (Fig. 6).

### Calculation Method

For the high-resolution and large-scale calculation of the pressure distribution, a contact model based on the half-space is used in combination with an optimized meshing strategy (method of combined solutions) [Ref.20]. The advantage of an analytical half-space model over a finite element analysis is the greatly reduced computational cost. Thus, the high-resolution pressure distribution in contact of real surface topographies as a result of a normal force can be calculated and analyzed for different rolling positions.

For the calculation of the variable pressure distribution, the rotation of the topography data is necessary after each pressure calculation of a rollingsliding position. Using different angles of rotation between the test and counter disk, a slip between the two contact surfaces can be mapped so that the angle of rotation of the counter disk  $\Delta\alpha_{CS}$  is greater than the angle of rotation of the test disk  $\Delta\alpha_{PS}$  in the case of negative slip from the point of view of the test disk. Figure 6 schematically shows the method

for calculating the change in the pressure distribution. The line contact between two cylindrical disks is analyzed. The area of interest is meshed with a fine mesh of rectangular elements. The remaining area of the macroscopic contact region is meshed with a coarser resolution to account for the interactions and to reduce the computational effort. For the pressure calculation, the stationary pressure distribution on the test disk is considered. To observe the change in the pressure distribution, the finely meshed area is shifted in the Y-direction in conjunction with the topography of the test disk (Fig. 6).

### Changing Pressure Distribution

Figure 7 shows the discretized pressure curves for a partial range of the load change on the test topography. For the contact calculation, a purely elastic material behavior is assumed, so that high pressures occur relative to an elastic-plastic material behavior for the investigation of the pressure distribution. The force equilibrium of the elastic contact calculation is calculated for the examination of the pressure distribution on the present cutout with an area of  $500\mu\text{m} \times 50\mu\text{m}$ . Thus, the cutout transmits the same normal force for all three variants.

The pressure distribution of a section of the macroscopic line pressure distribution for five rollingsliding positions (WS) is shown. Between the two topographies, the slip  $s_{\text{test}} = -100\%$  in relation to the test surface, so that a rotation angle per rollingsliding position of  $\Delta\alpha_{WS,\text{test}} = 0.0135^\circ$  results in a sliding distance of  $\Delta s_{\text{slip,counter}} = 5\mu\text{m}$ . To investigate the influence of different surface structures, three variants are compared with each other. The three variants result from different combinations of the orientation of the grinding grooves. In the case of the surface with transverse grinding, the grinding grooves run in the direction of the axis of rotation (axial), and in the case of the surface with circumference grinding, the grinding grooves run in the circumferential direction and thus in the direction of the frictional force.

A comparison of the pressure distribution curves between the

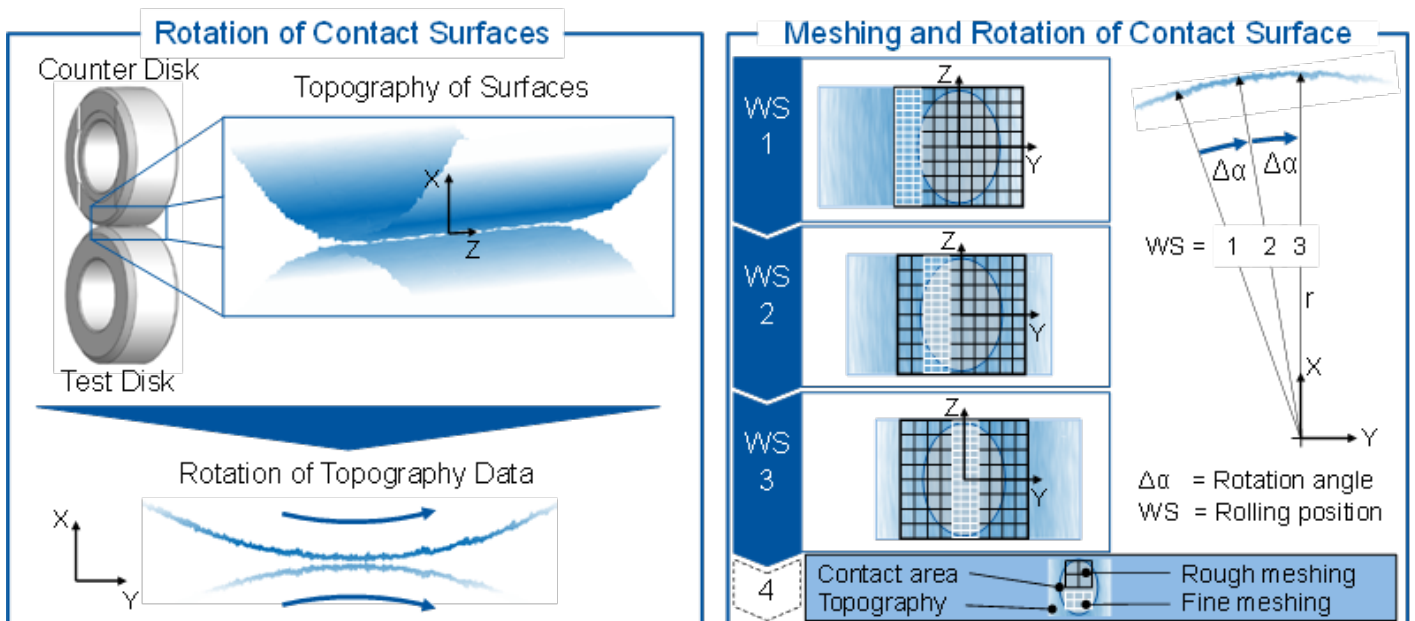


Figure 6 Calculation method of changing pressure distribution within dry rolling contacts.

variants with different grinding groove orientations (see Fig. 7) reveals significant differences. Variant 1 shows a section of the pressure distribution from the contact of transversely ground surfaces. The bending contact line that can be seen in rolling positions WS1 to WS3 results from the stochastic distribution of the roughness peaks and the topographic measurement of the surface. The characteristic picture of the pressure distributions of variant 1 changes with each rolling-sliding position. Here it can be seen that for individual micro contacts there are several contact changes within the macroscopic contact area. In contrast, the pressure distribution of variant 2 exhibits an approximately constant contact pattern for all rolling-sliding positions. Variant 3 shows the contact pattern from the contact between a transversely ground and a circumference ground surface. Here, on the one hand, areas can be seen which have contact with the opposite topography over all rolling-sliding positions. On the other hand, moving areas can be seen across the rolling-sliding positions, which can be traced back to the transversely ground surface structure of the counter disk. A contact change within the macroscopic load change interrupts the friction-induced energy supply, so that the local heat input is reduced. Thus, the contact changes simultaneously have a positive effect on the local temperature gradients and the service life of the contact.

### Local Frictional Energy

The advantage of a uniform distribution of the microscopic contact areas over all rollingsliding positions can be illustrated with the local friction-related energy conversion. If the entire contact is considered macroscopically, the friction-related average energy conversion can be calculated according to Equation 1 [Ref. 19]. For the calculation of the microscopic distribution of the friction energy, the normal force  $F_N$  can be calculated from a sum of the pressures and the edge lengths  $dz$  and  $dy$  of all elements according to Equation 2.

Figure 8 shows the summed frictional energy over all 5 rollingsliding positions of the 3 variants for a section of the

macroscopic contact area. Analogous to the pressure distribution, the distribution of the friction-related energy conversion also shows a more uniform distribution for variants 1 and 3. However, variant 2 exhibits higher local friction energies due to

$$E_R = \mu \cdot F_N \cdot s_{slip} \quad (1)$$

$E_R$	[Nm]	Frictional Energy
$F_N$	[N]	Normal Force
$\mu$	[-]	Friction Coefficient
$s_{slip}$	[m]	Slide Path

$$F_N = \sum_{i=1}^n p_i \cdot dy \cdot dz \quad (2)$$

$F_N$	[N]	Normal Force
$dy$	[mm]	Edge Length of Element in y
$n$	[-]	Number of Elements
$p_i$	[N/mm <sup>2</sup> ]	Pressure of Element i
$dz$	[mm]	Edge Length of Element in z

the approximately constant contact pattern over all rollingsliding positions, although the local pressures of variants 1 and 3 are greater.

In addition to the summed friction energy, Figure 8 shows the friction energy of a characteristic element with edge length  $dy = 1 \mu\text{m}$  and  $dz = 5 \mu\text{m}$  over the contact distance for the contact between two transversely ground surface structures. The two diagrams show the frictional energy conversion of a single element over the entire macroscopic contact distance of  $l_{\text{contact}} = 0.4 \text{ mm}$ . The frictional energy is shown with a resolution of 80 rolling-sliding positions over the entire contact distance. For the calculation of the friction energy curves, the pressure is considered constant over the increment of the sliding distance  $\Delta s_{\text{slip}}$ . The upper diagram shows the frictional energy curve for a slip of  $s_{\text{test}} = -10 \%$  and a resulting slip path of  $\Delta s_{\text{slip}} = 0.5 \mu\text{m}$  per

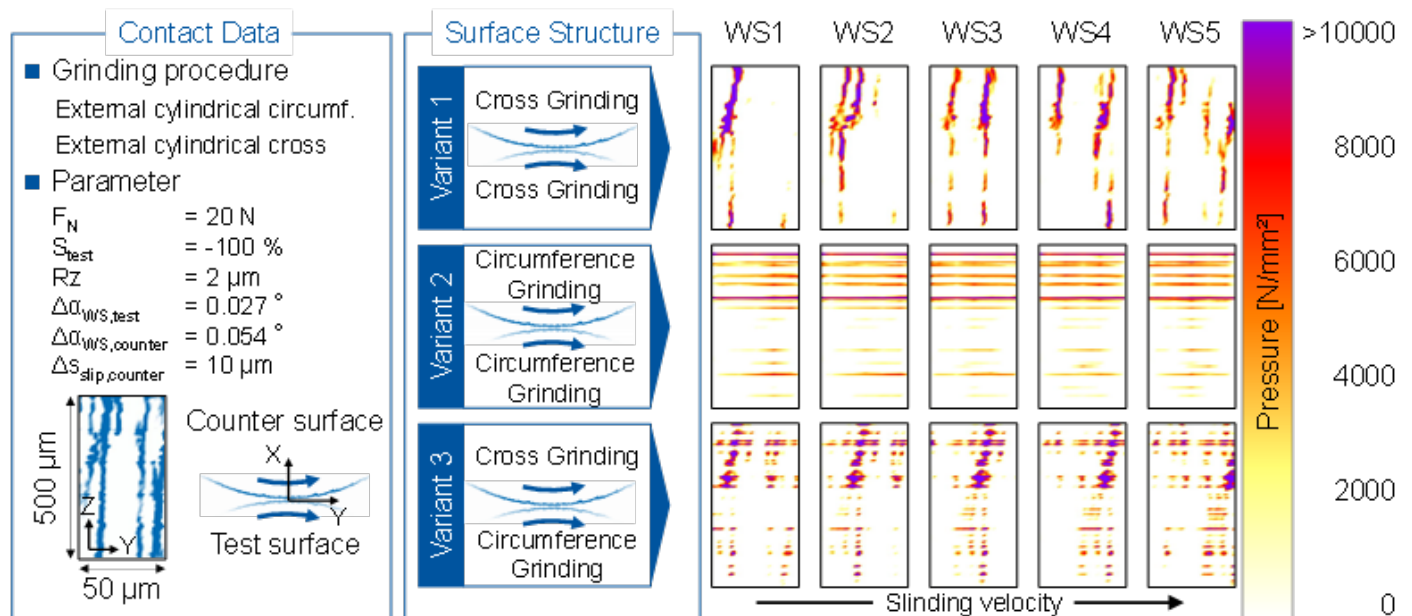


Figure 7 Pressure distribution depending on the contact position and surface structure.

rollingsliding position. The frictional energy curve shows that the microscopic element under consideration is in contact with the opposing topography three times over the contact distance. For a slip of  $s_{test} = -28\%$ , this results in a higher number of contact changes. The three contact phases from the upper diagram are therefore also the first three contact phases in the lower diagram. A comparison of the first contact phase in each case shows that a higher amount of frictional energy is mapped due to the greater sliding distance  $\Delta s_{slip}$ . In addition, further contact phases are added within the contact distance at higher slip.

Overall, a contact model exists which is suitable as a basis for a prediction model for the prediction of the coating wear and the service life taking into account thermal effects depending on the number of load cycles for the fluid-free contact of coated surfaces. With the assumption that the total frictional energy in the dry rollingsliding contact is converted into heat [Ref. 19], the method for calculating the local frictional energy provides a basis for considering thermal effects in the contact model. Furthermore, using the spatial and temporal distribution of the frictional energy, a method for calculating the layer wear can be implemented and developed for application to the dry contact.

### Summary and Outlook

The reduction of the friction coefficient and wear in most rolling contacts like the tooth contact in a gear box is achieved by the usage of a fluid lubrication system with oil or grease. The production and maintenance of these systems produce high costs. Furthermore, specific circumstances like vacuum or a high pressure range lead to instability of the properties of fluid lubricants. From this perspective a dry lubrication is necessary for many applications because a fluid lubrication system is not feasible. The conventional lubrication system has two primary functions. First, the reduction of the friction coefficient by separating the rolling surfaces, and second, the removal of the heat from the contact zone and the system. Secondary functions are the removal of particles from the contact zone and the

protection of the surfaces against corrosion. To optimize the dry lubricated rolling contact, three different approaches can be used: the gearing geometry, the core material of the gears, and the coating of the contacting surfaces. The objective of this report is the knowledge regarding the deficits of the dimensioning and the analysis of the dry lubricated rolling contact. Furthermore, the changing pressure distribution within a rolling contact of rough surfaces is analyzed.

The state of the art of dimensioning the gearing for dry lubricated rolling-sliding contact shows that current methods within the standardized guidelines for the calculation of the load capacity are not valid for dry lubrication with high mechanical load. The characteristics of the damage pattern from dry lubricated contact are similar to the characteristics of a scuffing damage. But for experimental analysis no uniform testing method is available. Pre-tests on the WZL disk-on-disk friction test rig show that the test rig and the testing procedure for scuffing are suitable for experimental investigations on the dry lubricated rolling contact. To reduce the costs of testing specimens and test rig capacity, prediction models are used to forecast the wear behavior and load capacity of gears and machining tools. There is a prediction model to forecast the wear of coated tooth flanks in fluid lubricated contact. The application of this prediction model on the dry lubricated rolling contact requires high resolution in order to take the whole contact area into account to consider thermal effects.

In order to forecast the wear behavior in a dry lubricated rolling contact, a method for the calculation of the changing pressure distribution is presented. The contact patterns of the three variants with different surface structure show that the combination of the two surface structures affect the changing behavior of the pressure distribution. The distributions of the frictional energy show the influence on the thermal effects within the contact area. To forecast the wear behavior considering thermal effects, experimental data from investigations on the test rig are required in the future. ⚙️

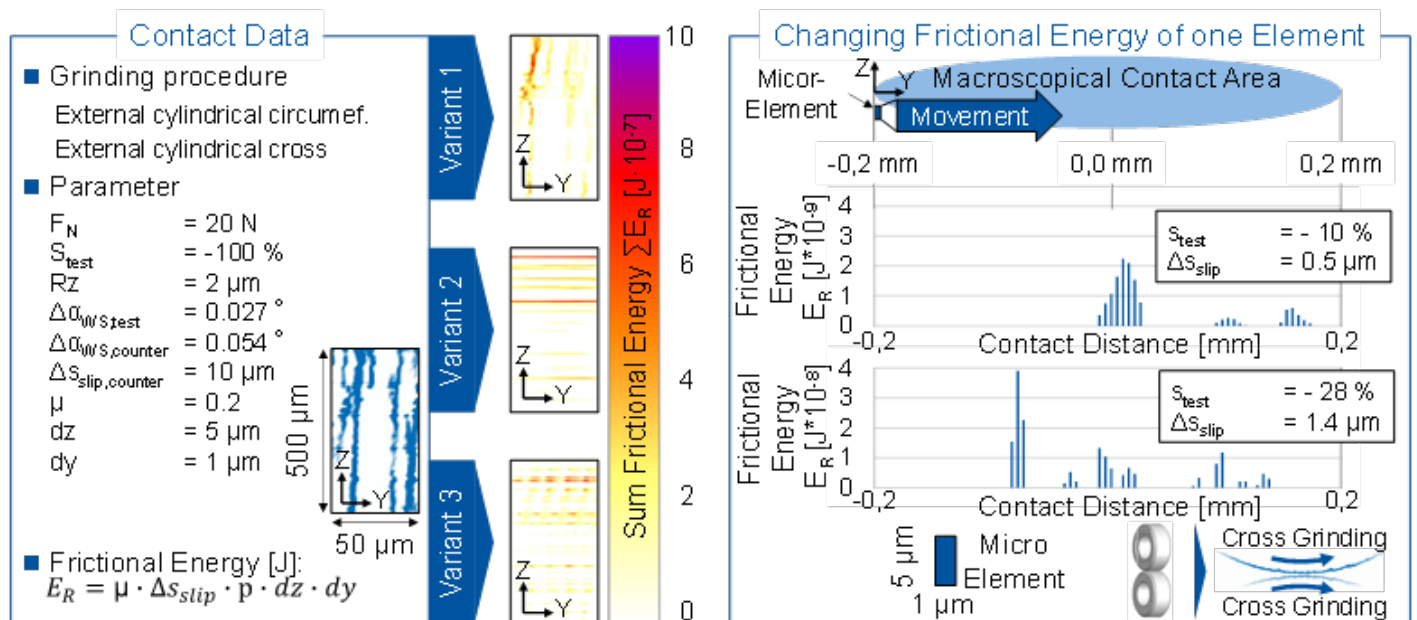
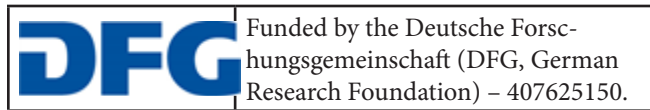


Figure 8 Distribution and history of the local frictional energy.

## Funding



## References

1. Sommer, K., R. Heinz and J. Schöfer. *Verschleiß metallischer Werkstoffe: Erscheinungsformen sicher beurteilen*. 1st ed. Wiesbaden: Vieweg + Teubner; 2010.
2. Klocke, F. and C. Brecher. *Zahnrad- und Getriebetechnik: Auslegung - Herstellung - Untersuchung - Simulation*. 1st ed. München: Hanser; 2017.
3. Krieger, H., D. Günther and I. Römhild. Studie zur Untersuchung von Minimalmengenschmierung und Trockenlauf für Getriebe: Studie. Studie. München; 1999.
4. Europäisches Parlament. *Maschinenrichtlinie 2006/42/EG*; 2006.
5. Hantschack, F. *Trockenlaufende Stirnräder in der Raumfahrt*. Würzburg; 2012.
6. Isaacson, A.C. and M.E. Wagner. "Oil-Off Characterization Method Using In-Situ Friction Measurement for Gears Operating Under Loss-of-Lubrication Conditions," *Gear Technology* 2019; June 2019:46–54.
7. Höhn, B.-R., A. Grossl, M. Diesselberg and S. Martens. "Development of Powertrain and Drive Line Components without Liquid Lubrication," Abschlussbericht. München; 2005.
8. Höhn, B.-R. and K. Michaelis (eds.). *Low Friction Powertrain: Tragfähigkeit Low Loss Verzahnung*. Frankfurt am Main: FVA (Forschungsvereinigung Antriebstechnik e.V.); 2013.
9. Schultz. Nitrierte Stahlzahnäder trotz dem Verschleiß. VDI Nachrichten 1986(18):20.
10. Hornbogen, E., G. Eggeler and E. Werner. *Werkstoffe: Aufbau und Eigenschaften von Keramik-, Metall-, Polymer- und Verbundwerkstoffen*. 10th ed. Berlin: Springer; 2012.
11. Miyoshi, K. (ed.). "Solid Lubricants and Coatings for Extreme Environments: State-of-the-Art Survey," Cleveland, Ohio: Glenn Research Center; 2007.
12. Brecher, C., C. Gorgels and A. Bagh. *Improvement of the Efficiency of Parallel-Axis Transmissions by Means of PVD-Coatings*, Weinheim: Wiley-VCH Verlag; 2009.
13. Brecher, C., H. Schlattmeier and C. Bugiel. "Load Carrying Capacity of PVD-coated Gearings," *Gear Industry Journal* 2004;1(2):48–52.
14. Yilmaz, M., D. Kratzer, T. Lohnner, K. Michaelis and K. Stahl. "A study on highly-loaded contacts under dry lubrication for gear applications," *Tribology International* 2018(128):410–20.
15. Norm. Zahnäder. FZG-Prüfverfahren. FZG-Prüfverfahren A/8,3/90 zur Bestimmung der relativen Fresstragfähigkeit von Schmierölen (14635 Teil 1). Berlin: Beuth; 2006.
16. Kropp, J.-P. and M. Petrik (eds.). *Optimierte Stahlzahnäder für Minimalmengenschmierung oder Trockenlauf: Abschlussbericht für AiF-Vorhaben Nr. 13745 N. Braunschweig*; 2006.
17. Greschert, R. „Ausbildung tragfähigkeitssteigernder Grenzschichten in der Zahnradfertigung," Diss. Aachen; 2019.
18. Popov, V. *Kontaktmechanik und Reibung: Von der Nanotribologie bis zur Erdbebedynamik*. Berlin: Springer; 2010.
19. Czichos, H. and K.-H. Habig. *Tribologie-Handbuch: Tribometrie, Tribomaterialien, Tribotechnik*. 3rd ed. Wiesbaden: Vieweg + Teubner; 2010.
20. Brecher, C., D. Renkens and C. Löpenhaus. "Method for Calculating Normal Pressure Distribution of High Resolution and Large Contact Area," *J. Tribol.* 2016;138(1):011402-1 - 011402-9.

**Sebastian Sklenak** joined Laboratory for Machine Tools and Production Engineering (WZL) of RWTH Aachen University in 2017, where he works as a Research Assistant in Gear Technology. As a Research Assistant, Sebastian works in the Gear Power Density group and works on projects related to the investigation of tooth flank and tooth root load capacity of gears using experimental analogy tests. Currently he is pursuing his Ph.D. in Mechanical Engineering, with a focus on Tribological Operation Behavior and Service Life Calculation in PVD-Coated and Dry Lubricated Tooth Contact of Gears. He holds a B.Eng. and M.Eng. in Mechanical Engineering from FH Aachen University of Applied Sciences. In his master thesis, he developed a Method for Calculating Plastic Deformation of High Resolution and Large Contact Area for Dry Lubricated Rolling Contacts. Prior to joining the University, Sebastian completed an apprenticeship as a bicycle mechanic including maintenance of bicycle gear hubs.



**Dr.-Ing. Jens Brimmers** is the head of the gear department at the Laboratory for Machine Tools and Production Engineering (WZL) of RWTH Aachen University since June 2019. He graduated from RWTH Aachen University with master's degrees in mechanical engineering and business administration. His Ph.D. thesis focused on beveloid gears and topological tooth flank modification.



**Prof. Dr.-Ing. Christian Brecher** has since January 2004 been Ordinary Professor for Machine Tools at the Laboratory for Machine Tools and Production Engineering (WZL) of the RWTH Aachen, as well as Director of the Department for Production Machines at the Fraunhofer Institute for Production Technology IPT. Upon finishing his academic studies in mechanical engineering, Brecher started his professional career first as a research assistant and later as team leader in the department for machine investigation and evaluation at the WZL. From 1999 to April 2001, he was responsible for the department of machine tools in his capacity as a Senior Engineer. After a short spell as a consultant in the aviation industry, Professor Brecher was appointed in August 2001 as the Director for Development at the DS Technologie Werkzeugmaschinenbau GmbH, Mönchengladbach, where he was responsible for construction and development until December 2003. Brecher has received numerous honors and awards, including the Springorum Commemorative Coin; the Borchers Medal of the RWTH Aachen; the Scholarship Award of the Association of German Tool Manufacturers (Verein Deutscher Werkzeugmaschinenfabriken VDW); and the Otto Kienzle Memorial Coin of the Scientific Society for Production Technology (Wissenschaftliche Gesellschaft für Produktionstechnik WGP).

